Journal of Inflammation Research

Dovepress
open access to scientific and medical research

Open Access Full Text Article

ORIGINAL RESEARCH

Chitosan/Sodium Alginate/Velvet Antler Blood Peptides Hydrogel Promotes Diabetic Wound Healing via Regulating Angiogenesis, Inflammatory Response and Skin Flora

Mingqian Hao[1,2,*], Chuanbo Ding[1,*], Shuwen Sun[2], Xiaojuan Peng[2], Wencong Liu[2]

[1]College of Traditional Chinese Medicine, Jilin Agricultural Science and Technology College, Jilin, People's Republic of China; [2]School of Chinese Medicinal Materials, Jilin Agricultural University, Changchun, People's Republic of China

*These authors contributed equally to this work

Correspondence: Chuanbo Ding, College of Traditional Chinese Medicine, Jilin Agricultural Science and Technology College, Jilin, 132109, People's Republic of China, Tel +8615948721648, Email chuanboding0506@163.com; Wencong Liu, School of Chinese Medicinal Materials, Jilin Agricultural University, Changchun, 130118, People's Republic of China, Tel +8613804460499, Email jwlw6803@126.com

Background: Diabetic ulcer remains a clinical challenge due to impaired angiogenesis and persistent inflammation, requiring new alternative therapies to promote tissue regeneration.

Purpose: In this study, chitosan/sodium alginate/velvet antler blood peptides (CS/SA/VBPs) hydrogel (CAVBPH) was fabricated and used in the treatment of skin wounds in type 2 diabetes mellitus (T2D) for the first time.

Methods: VBPs were prepared by hydrolysis and ultrafiltration, and their sequences were identified using LC-MS/MS. The CAVBPH was further fabricated and characterized. A mouse model of T2D was induced by a high-sugar and high-fat diet (HSFD) and streptozotocin (STZ) injection. CAVBPH was applied topically to T2D wounds, and its effects on skin repair and potential biological mechanisms were analyzed by appearance observation, histopathological staining, bioinformatics analysis, Western blot, and 16S rRNA sequencing.

Results: VBPs had numerous short-chain active peptides, excellent antioxidant activity, and a low hemolysis rate. CAVBPH exhibited desirable biochemical properties and participated in the diabetic wound healing process by promoting cell proliferation (PCNA and α-SMA) and angiogenesis (capillaries and CD31) and alleviating inflammation (CD68). Mechanistically, the therapeutic effect of CAVBPH on chronic wounds might rely on activating the PI3K/AKT/mTOR/HIF-1α/VEGFA pathway and reversing the expression of inflammatory cytokines TNF-α and IL-1β. The results of 16S rRNA sequencing indicated that T2D significantly altered the diversity and structure of skin flora at the wound site. CAVBPH treatment elevated the relative abundance of beneficial microbes (e.g., *Corynebacterium_1* and *Lactobacillus*) and reversed the structural imbalance of skin microbiota.

Conclusion: These results indicate that CAVBPH is a promising wound dressing, and its repair effect on diabetic wounds by regulating angiogenesis, inflammatory response, and skin flora may depend on the rich small peptides in VBPs.

Keywords: velvet antler blood peptides, diabetic wound, hydrogel, bioinformatics, skin flora

Introduction

Diabetes mellitus is a common chronic metabolic disease, typically manifested as metabolic disorders and hyperglycemia, and its incidence is expected to increase to 592 million patients by 2035.[1,2] 15–25% of diabetic patients have non-healing skin wounds, such as foot ulcers (DFU), which are usually in a stage of chronic inflammation rather than a series of repairing events, and further pose gangrene, amputation and even death.[3] Because traditional therapies and the exploration of underlying mechanisms are usually inadequate, more effective clinical treatment strategies to promote diabetic wound healing are desired.[4–7]

Received: 9 June 2022
Accepted: 18 August 2022
Published: 26 August 2022

Uncovered diabetic wounds often display persistent hyperglycemia and immune dysregulation, and are susceptible to bacterial invasion. Predictably, these aforementioned conditions further aggravate the inflammatory response, skin ulcers, and healing impairments.[8] Therefore, the treatment of diabetic wounds requires dressings with multiple functions such as good hygroscopicity, drug delivery ability, biodegradability, antibacterial effect, anti-inflammatory activity, and antioxidant capability to overcome the limitations of traditional therapy.[9] Hydrogels are becoming an attractive option in creating environments for promoting wound healing due to their skin-mimicking structure and excellent biochemical characteristics. As natural polysaccharides, chitosan (CS) and sodium alginate (SA) are widely applied in the field of tissue engineering, especially in the development of wound dressings.[10–12] CS/β-glycerophosphate sodium (β-GP) hydrogel systems have good temperature sensitivity and biocompatibility, which are beneficial to drug release, cell proliferation, and tissue repair and have been utilized in ocular treatment, periodontal repair, and skin trauma at present.[13–15] Alginate biomaterial can also enhance granulation tissue formation and wound healing.[12] Hence, the combination of biopolymers with healing potential may provide an opportunity to synthesize wound dressings that stimulate skin repair.

The previously reported CS-based oyster peptide microsphere thermosensitive hydrogel promoted skin wound repair in mice via up-regulating the expression of Ki-67 and VEGF and suppressing inflammatory cytokines.[16] Wei et al fabricated a CS/alginate hydrogel loaded with FGF/VE-cadherin and evaluated its potential as a wound dressing for repairing defective skin.[17] In addition, hydroxypropyl cellulose/SA hydrogel loaded with antibacterial peptide NZ2114 was confirmed to accelerate wound healing by promoting the expression of VEGF, EGF, and CD31 as well as reducing inflammatory response.[18] These studies demonstrate that hydrogels encapsulating bioactive peptides/proteins seem to be a promising research direction for wound dressings. However, it is currently insufficient to deeply explore the biological mechanism by which hydrogels accelerate wound repair.

In recent years, animal-derived small peptides, including velvet antler peptides, oyster peptides, chum salmon peptides, and tilapia peptides, have been found to have not only antibacterial, anti-inflammatory, and antioxidant properties but also skin care and tissue repair functions.[16,19–21] Velvet antler blood (VB) is the blood extracted from freshly collected velvet antler and has been recorded as a traditional Chinese medicine for restoring and tonifying in Chinese medical classics Shen Nong Ben Cao Jing 2000 years ago.[22] VB is rich in protein, providing the material basis for the growth and restoration of velvet antler. It was previously found that velvet antler blood peptides (VBPs), the major components of VB, have significant anti-fatigue and antioxidant effects, yet, it is still unknown whether VBPs are a crucial factor for tissue repair.[23,24]

Based on the above characteristics, in this study, we fabricated a CS/SA thermosensitive hydrogel loaded with VBPs (CAVBPH) and further explored its effects on diabetic wounds and skin flora. To the best of our knowledge, this is the first comprehensive exploration of the underlying biological mechanisms of CAVBPH for diabetic wound healing.

Materials and Methods

Materials

Freeze-dried VB powder was obtained from Jinlu Pharmaceutical Co., Ltd. (Changchun, China). SA (molecular weight of 32–250 kDa) and CS (deacetylation degree of 95%, viscosity of 200–400 mPa·s) were purchased from Meryer Chemical Technology Co., Ltd. (Shanghai, China). β-GP was purchased from Yuanye Bio-Technology Co., Ltd. (Shanghai, China). Streptozocin (STZ) and chloral hydrate were, respectively, from Sigma-Aldrich Co., Ltd. (Shanghai, China) and Fuchen Chemical Reagent Factory (Tianjin, China). BCA protein assay kit (P0010) and RIPA lysis buffer (P0013B) were obtained from Beyotime (Shanghai, China). HaCat cells were from Cellcook Biotech Co., Ltd. (Guangzhou, China). All other agents were of analytical grade.

Preparation and Characterization of VBPs

VBPs were prepared using in vitro simulated gastrointestinal digestion and ultrafiltration technique as previously reported.[25] Peptide sequences were identified and analyzed by utilizing the Ultimate 3000 high-performance liquid chromatography system (HPLC, Thermo Fisher Scientific, USA) coupled with a Q Exactive™ Hybrid Quadrupole-Orbitrap™ Mass Spectrometer (Thermo Fisher Scientific, USA) with an ESI nanospray source.

Preparation of CAVBPH

First, 2% w/v CS solution was prepared in the acetic acid solution (0.1 M, 10 mL), and 2.5 mL of 56% w/v β-GP solution was dripped into the cold CS solution and fully mixed. Then, 0.1 g SA was added to the CS/β-GP solution, and 0.2 mL of 0.5% w/v $CaCl_2$ solution was added dropwise to the mixture to prepare CS/β-GP/SA/Ca^{2+} hydrogel (CAH). Subsequently, VBPs were introduced into CAH scaffold and CAVBPH with peptides concentration of 1 mg/mL was fabricated. The gelation behavior of CAH and CAVBPH was evaluated via the glass vial dumping test at 37 °C. 5 mL of CAH solution or CAVBPH solution transitioned from sol to gel within 5 min at this controlled temperature, indicating that hydrogels possessed good temperature sensitivity. The solutions mentioned above were freshly prepared and kept at 4 °C before use.

In vitro Characterization of Hydrogels

The microstructure of freeze-dried hydrogel was analyzed by scanning electron microscope (SEM; SS-550, Shimadzu, Japan). Infrared (IR) spectra were detected using an FTIR spectrometer (FTIR-650, Gangdong, China). Subsequently, the swelling behaviors and in vitro biodegradation profiles of samples were, respectively, investigated according to previous reports.[26,27] The release profile of VBPs was further plotted. Briefly, lyophilized CAVBPH (W_0) was immersed in 10 mL of PBS with constant shaking. At regular intervals, 1 mL of the co-incubated solution was replaced by the same volume of freshly prepared PBS. The release of VBPs was analyzed utilizing BCA protein assay kit according to the manufacturer's instructions.

Antioxidant and Biosafety Assays

Hydrogels were soaked in PBS for 24 h to prepare the extraction solutions (1 mg/mL), and GSH and VBPs were used as the positive control. Antioxidant ability of CAH and CAVBPH was evaluated via DPPH and ABTS radical scavenging assays according to a previous study.[28] Meanwhile, 1% w/v TritonX-100 solution and PBS were, respectively, prepared as the positive control and negative control, and the hemolysis rate was determined according to the reference.[26] HaCaT cells were selected to test the cytotoxicity of hydrogel samples. UV-sterilized CAH or CAVBPH was immersed in the culture medium for 24 h to prepare the hydrogel extract medium. And HaCaT cells culture and cell viability assay (MTT method) were performed as previously described.[29]

Bioinformatics Analysis

The dataset of diabetic skin wounds (GSE147890) based on the GPL571 platform was downloaded from the Gene Expression Omnibus database (https://www.ncbi.nlm.nih.gov/geo/). Dataset GSE147890 contains 5 intact normal skin samples (C0h), 7 intact diabetic skin samples (D0h), 6 acute wounds samples 24 h after operation (C24h), and 6 diabetic wounds samples 24 h after operation (D24h). The DEGs of acute wound (C24h vs C0h) and diabetic wound (D24h vs D0h) were identified with the threshold of $|\log2FC| > 1$ and $p < 0.05$ by utilizing the limma package within the R language environment (version 3.6.2).[30] The overlapping DEGs of acute wounds and diabetic wounds and the specific DEGs of diabetic wounds were identified utilizing the Jvenn plugin (http://www.bioinformatics.com.cn/static/others/jvenn/). Subsequently, the roles of overlapping DEGs and specific DEGs were evaluated on the DAVID Bioinformatics Resources platform (https://david.ncifcrf.gov/).

Animal Experiment for Wound Healing

ICR male mice (18–22 g) came from Yisi Experimental Animal Technology Co., Ltd. (Certificate No. SCXK-2020-0001, Changchun, China) and were fed in a standard laboratory environment (22 ± 2 °C, 60 ± 5% humidity, and a 12 h light/12 h dark cycle). All experimental procedures were approved by the Animal Care and Use Committee of Jilin Agricultural University and strictly followed the NIH Guide for the Care and Use of Laboratory Animals.

Type 2 diabetes mellitus (T2D) in mice was induced as previously reported.[31] After one week of adaptive feeding, the normal control (NC) group was fed a normal diet, while the other mice were fed a high-sugar and high-fat diet (HSFD; basic food 49.5%, sucrose 25%, lard oil 15%, milk powder 5%, yolk powder 5%, and sodium cholate 0.5%) for 31 days (Figure S1A). HSFD mice were fasted for 12 h before intraperitoneal injection (i.p.) with STZ in citric acid buffer (0.1 M, pH 4.3) daily for 3 days (80, 70, and 60 mg/kg, successively), whereas NC mice were injected with vehicle solution. Mice with fasting blood glucose (FBG) ≥ 11.1 mM and typical clinical polydipsia, polyphagia, polyuria, and weight loss after one week were considered T2D.

On the day of surgery, all mice were treated with chloral hydrate (400 mg/kg, i.p.) and a full-thickness circular wound with a radius of 0.5 cm was induced when hair was removed from the dorsal region. The T2D animals with wounds were randomly divided into 3 groups (n = 12/group): the T2D group, the CAH group, and the CAVBPH group. The NC and T2D groups were treated with 0.2 mL of PBS, while the CAH and CAVBPH groups received the same volume of CAH and CAVBPH treatment, respectively. Wound size was observed on days 0, 3, 9, and 15 post-surgery and the wound healing rate was determined using the Image J software.

Histopathological Analysis

The wound along with the surrounding new skin was fixed in 4% paraformaldehyde for 24 h and further processed for hematoxylin and eosin (H&E) staining, Masson's trichrome (Masson) staining, and immunohistochemical (IHC) staining. In this study, anti-CD31 (ab182981, Abcam), anti-CD68 (BA3638, BOSTER), anti-PCNA (BM0104, BOSTER), and anti-α-SMA (BM0002, BOSTER) reagents were used for IHC staining of tissue sections as previously described.[16] Images were obtained using a Nikon upright microscope (E100, Tokyo, Japan). The collagen content was analyzed using the Image J software and the integrated optical density (IOD) values of different proteins were identified by the Image-Pro Plus 6 software.

Western Blot

Skin wound tissues were harvested and homogenized in cold RIPA lysis buffer, and the supernatant of the sample was collected after centrifugation at 4 °C. BCA protein kit was used to measure protein concentration in different groups. Western blot analysis was performed for antibodies p-PI3K (#4228, Cell Signaling, China), PI3K (67071-1-lg, Proteintech, China), p-AKT (ARG51559, Arigobio, China), AKT (60203-2-lg, Proteintech, China), p-mTOR (ARG40666, Arigobio, China), mTOR (10745-1-AP, Proteintech, China), HIF-1α (20960-1-AP, Proteintech, China), VEGFA (19003-1-AP, Proteintech, China), IL-1β (26048-1-AP, Proteintech, China), TNF-α (17590-1-AP, Proteintech, China) and β-actin (66009-1-lg, Proteintech, China) as previously reported.[25] β-actin was used as an internal standard. The protein blots were visualized by enhanced chemiluminescent assay and quantified using the Image J software.

16S rRNA Sequencing of Skin Flora

Before the mice were euthanized on day 15, the skin microbial samples of each group (n = 10) were collected by gently swabbing the wound along with the surrounding new skin with sterile cotton swabs soaked in normal saline. 16S rRNA sequencing was performed by Shanghai Personal Biotechnology Co., Ltd. The outcomes were analyzed on the Gene cloud platform (https://www.genescloud.cn/home).

Statistical Analysis

Triplicate experiments were performed unless stated otherwise. Data are presented as mean ± standard deviation (SD). IBM SPSS Statistics 23 software was applied to compare the differences between groups by one-way analysis of variance with the LSD test. Spearman correlation coefficients between the composition of T2D wound microflora and the expression of active proteins were evaluated by utilizing the OmicStudio platform (https://www.omicstudio.cn/tool). $p < 0.05$ was considered statistically significant.

Results

VBPs Contained Abundant Short-Chain Peptides

LC-MS/MS results showed that 89.78% of VBPs had a molecular weight of less than 1 kDa. VBPs had 372 sequences (LKECCDKPV, VGYP, LFP, EHF, FPH, etc.), 96.5% of them were short-chain peptides (no more than 10 amino acids) (Table S1). Only very few sequences have been found with anti-ACE, antibacterial, and antioxidant activities in the BIOPEP database (https://biochemia.uwm.edu.pl/biopep/start_biopep.php), and the bioactivities of most peptides remain unknown.

Hydrogel Had Excellent in vitro Physicochemical Properties

The preparation process of CAVBPH was shown in Figure 1A. Hydrogel maintained liquid at room temperature and transformed into gel when the temperature increased to human body temperature. The interaction between CS and β-GP mainly involved intermolecular hydrogen bonds and electrostatic effect, and the eggshell-like cross-linked structure between SA and Ca^{2+} also improved the mechanical properties of hydrogel. All hydrogels had a highly porous structure at the microscopic level and the introduction of VBPs did not make a difference in the structure of porosity (Figure 1B), which not only built an environment for cell attachment and migration but also satisfied gas exchange of the wound bed.

The IR spectra were presented in Figure 1C. In the IR spectra of CAH and CAVBPH, the N-H vibration absorption peak (1568 cm^{-1}) of $-NH_3^+$ in CS molecule and the asymmetric and symmetric stretching vibration peaks (1082 and 973 cm^{-1}) of PO_4^{3-} in β-GP molecule were obviously weakened, showing that electrostatic effect occurred between $-NH_3^+$ and PO_4^{3-}.[16,21] The stretching vibration of C=O (1633 and 1420 cm^{-1}) and C-O (1032 cm^{-1}) and the deformation vibration of O-H (1320 cm^{-1}) associated with SA in hydrogel were weakened when cross-linked with Ca^{2+}.[32] For VBPs, the absorption peaks at 1630 and 1582 cm^{-1} corresponded to the characteristic parameters of amide I and II, respectively; the bands at 1455, 1404, and 1111 cm^{-1} were, respectively, related to C-H bending vibration, O-H bending vibration, and C-O stretching vibration.[16,21] The IR spectrum of CAVBPH displayed obvious absorption bands of VBPs (1582 cm^{-1}, 1404 cm^{-1}, 1111 cm^{-1}, etc.), which suggested that VBPs have been loaded into the hydrogel.

Figure 1D showed that CAVBPH and CAH quickly absorbed water and achieved swelling ratios of over 200% within 1 h due to their hydrophilicity and interconnected porous structure, which was important to cover the wound and obtain a sustained drug delivery. Moreover, with the increase of incubation time, the mass residue of hydrogels gradually decreased (Figure 1E). On day 14, the residual weights of CAVBPH and CAH dropped from 100% to 59.26% and 56.85%, respectively. The appropriate anti-degradation performance of hydrogels also demonstrated their long-time covering and protective effects on wounds.

The three-dimensional porous structure of the dressing facilitates the rapid delivery of drugs or cells to the affected tissue. As presented in Figure 1F, CAVBPH showed a burst release with a release amount of 44.80% within 12 h, indicating the low molecular weight of short-chain peptides and the high porosity of CAVBPH might increase the diffusion coefficient of VBPs. VBPs in CAVBPH exhibited a nearly linear continuous release (74.79%) within 12–48 h. After 48 h, the release speed slowed down but this process was still maintained and reached 82.24% after 240 h, demonstrating that CAVBPH had desirable sustained release behavior.

Hydrogel Exerted Antioxidant Activity and Biosafety in vitro

An increasing number of reports have shown that skin dressings with antioxidant activity could improve the therapeutic effect for tissue repair.[33,34] In this study, CAH showed almost no antioxidant activity, DPPH and ABTS radicals scavenging abilities of CAVBPH were 10.97% and 45.81%, respectively, while the antioxidant activities of VBPs and GSH were superior to those of CAH and CAVBPH ($p < 0.001$), indicating that the antioxidant capacity of CAVBPH was related to the addition of VBPs (Figure 2A).

Wound dressings are usually indirect or direct contact with wounds and blood, so biocompatibility is regarded as a prerequisite for the clinical application of dressings. Dressings are generally considered clinically safe with a hemolysis rate of less than 5%.[35] The results showed that obvious hemolysis appeared in the positive control, but the hemolysis rates of VBPs, CAVBPH, and CAH were not more than 1.5% (Figure 2B). Cytotoxicity is an important index for the practical application of hydrogel dressings. The cell viability maintained almost unchanged with the increase of hydrogel concentration from 50 μg/mL to 500 μg/mL as presented in Figure 2C. The cell vitality of the CAH and CAVBPH groups was 81.29% and 86.74%, respectively, when the concentration was 5000 μg/mL. Samples with more than 75% cell viability are generally regarded as non-cytotoxic referring to ISO 10993–5: 1999 (GB/T 16886.5–2003).[36] Hence, CAH and CAVBPH are considered to possess negligible toxicity and good biosafety.

Bioinformatics Analysis of Acute Wound and Diabetic Wound

A total of 245 up- and 190 down-regulated DEGs were identified in acute skin wounds, and 609 DEGs (299 up- and 310 down-regulated) were found from diabetic skin wounds (Figure 3A and B). Besides, 339 overlapping DEGs between

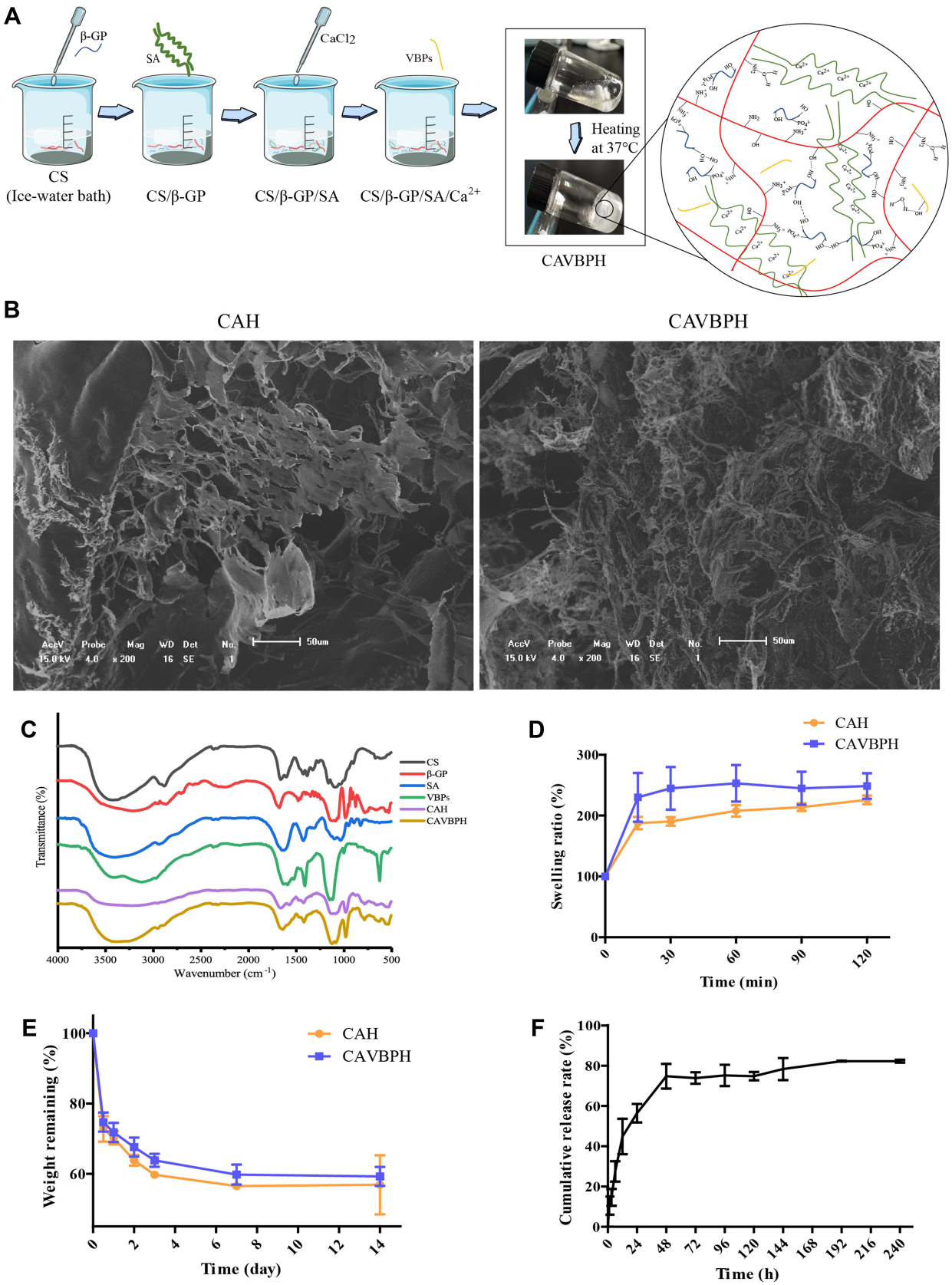

Figure 1 Preparation and in vitro performance evaluation of hydrogels. (**A**) The preparation process of hydrogels. (**B**) SEM micrograph (scale bar = 50 μm). (**C**) Infrared (IR) spectroscopy. (**D**) Swelling test. (**E**) Biodegradation test. (**F**) In vitro release profile of VBPs from CAVBPH.

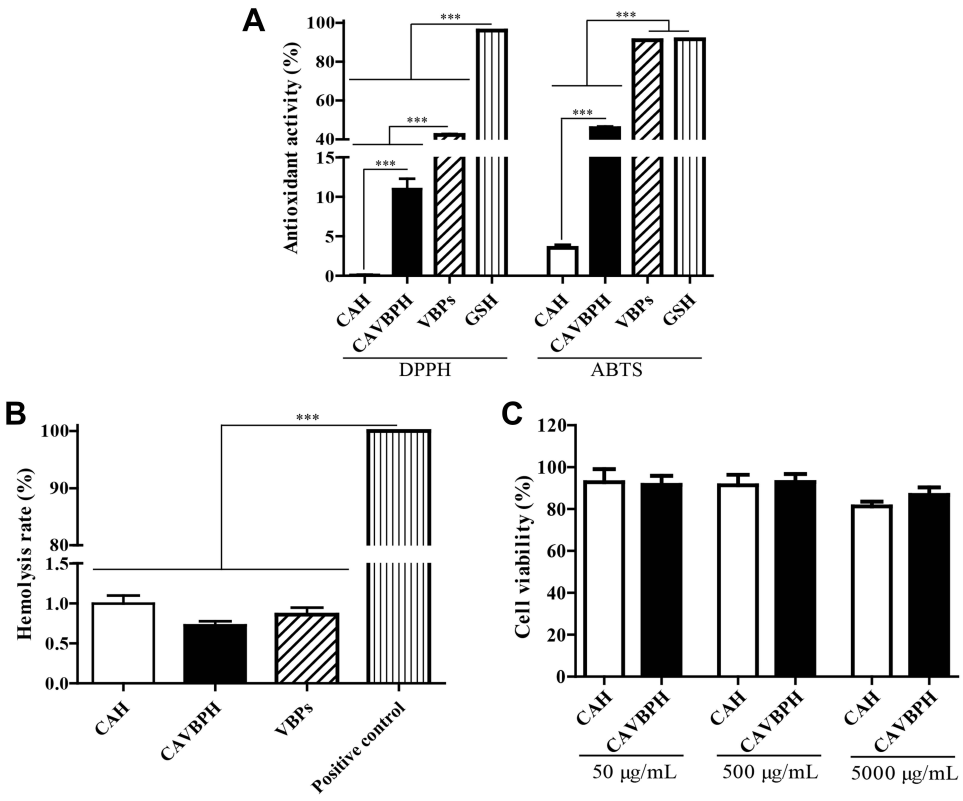

Figure 2 In vitro activity analysis of hydrogels. (**A**) DPPH and ABTS radicals scavenging activities. (**B**) Hemolysis test. (**C**) Cell viability test. ***$p < 0.001$.

acute skin wounds and diabetic skin wounds (199 up- and 140 down-regulated) and 270 specific DEGs of diabetic skin wounds (100 up- and 170 down-regulated) were obtained through Venn diagram analysis (Figure 3C).

As shown in Figure 3D, Gene Ontology-biological processes (GO-BP) of overlapping DEGs were mainly enriched in cell adhesion, positive regulation of cell proliferation, neutrophil degranulation, and inflammatory response. The terms of overlapping DEGs in Kyoto Encyclopedia of Genes and Genomes (KEGG) were predominantly enriched in the PI3K-AKT signaling pathway, IL-17 signaling pathway, TNF signaling pathway, and NF-κB signaling pathway (Figure 3E). The BP category of specific DEGs in diabetic wounds was significantly related to positive regulation of transcription, negative regulation of apoptotic process, and positive regulation of gene expression (Figure 3F). In addition, the specific DEGs of diabetic wounds were predominantly enriched into the PI3K-AKT signaling pathway, cAMP signaling pathway, HIF-1 signaling pathway, and JAK-STAT signaling pathway (Figure 3G).

CAVBPH Accelerated T2D Wound Healing

During the in vivo experiment, T2D mice still maintained a higher FBG level than 11.1 mM and the typical symptoms of clinical polydipsia, polyphagia, polyuria, and weight loss after injection of STZ. As shown in Figure S1B, the pancreatic islets of NC mice showed normal architecture. In contrast, considerable degenerative changes in pancreatic islets were detected in T2D mice, including the size and number of islets decreased and islet β-cells damaged. All these results demonstrated that the stable T2D model has been successfully established.

As shown in Figure 4A, the wound size in all groups decreased gradually over time. Compared with the NC group, the T2D group displayed a slower wound shrinkage due to the influence of diabetes, and exudate was still found on the wound surface on day 9. Topical application of CAH and CAVBPH significantly accelerated diabetic wound recovery compared to the T2D group. Quantitative analysis of wound healing confirmed the above results (Figure 4B). The healing rate in the T2D group was less optimistic than that in the NC group ($p < 0.01$ or $p < 0.001$). Compared to the T2D group, the CAH group showed a better healing effect on days 9 and 15 ($p < 0.001$), while the CAVBPH group had the best

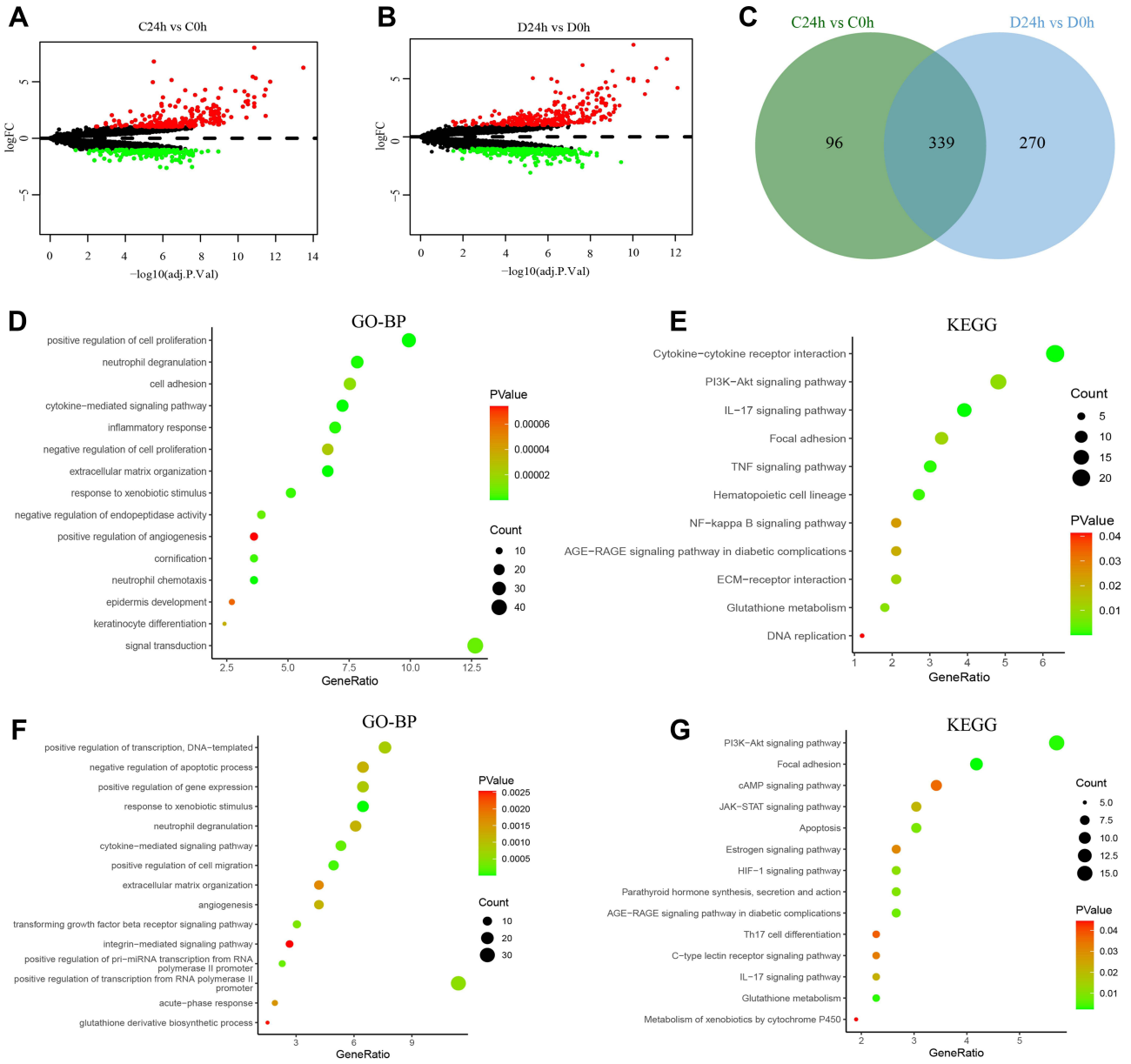

Figure 3 Bioinformatics analysis of acute skin wounds (C24h vs C0h) and diabetic skin wounds (D24h vs D0h). (**A** and **B**) Identification of DEGs in acute skin wounds and diabetic skin wounds, respectively. (**C**) Identification of overlapping DEGs between acute skin wounds and diabetic skin wounds, and the specific DEGs of diabetic skin wounds. (**D** and **E**) Gene Ontology-biological processes (GO-BP) and Kyoto Encyclopedia of Genes and Genomes (KEGG) enrichment analysis of overlapping DEGs. (**F** and **G**) GO and KEGG enrichment analysis of the specific DEGs.

wound shrinkage than the T2D and CAH groups on all observed days ($p < 0.01$ or $p < 0.001$). At day 15, the wounds of the CAVBPH group (96.55% of healing rate) and the NC group (91.77% of healing rate) were basically healed and covered with hair, while the healing rates of the CAH and T2D groups were 84.23% and 63.81%, respectively.

CAVBPH Promoted Remodeling of the Microstructure of Wound Tissue

Concerning microstructure, T2D wound showed necrosis, inflammatory cell infiltration, and no epidermis on day 15 (Figure 5A). Moreover, the T2D group had lower levels of granulation tissue and new capillaries than NC mice. As compared with the T2D group, the CAVBPH and CAH groups presented more regenerated epidermis, granulation tissue, and new capillaries but negligible inflammatory cell infiltration. We also found that the CAVBPH group had more mature proliferating cells and skin appendages than the CAH group. Masson staining results showed that the treatment of CAH and

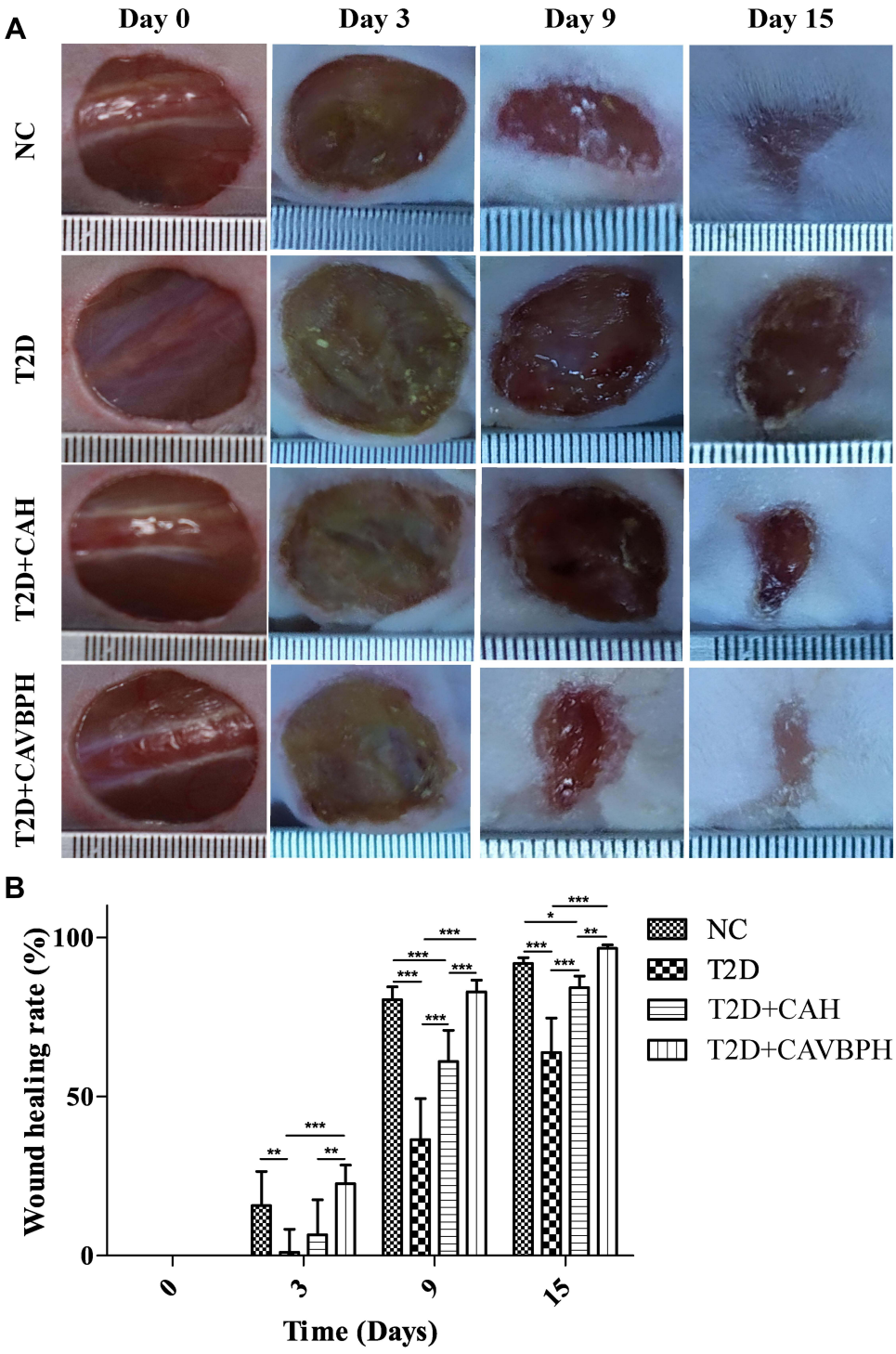

Figure 4 The effects of hydrogels on skin wound healing in type 2 diabetes mellitus (T2D) by topical treatment. (**A**) Representative images of wounds in the normal control (NC) group, T2D group, CAH (T2D+CAH) group, and CAVBPH (T2D+CAVBPH) group on days 0, 3, 9, and 15. (**B**) Wound healing rate. *$p < 0.05$, **$p < 0.01$, and ***$p < 0.001$.

CAVBPH increased collagen formation compared to the T2D group (Figure 5A). Notably, the collagen arrangement of the CAVBPH group was denser, ordered, and more mature than that of the CAH group. Quantitative analysis displayed that hydrogel treatment significantly increased collagen content in diabetic wounds ($p < 0.01$ or $p < 0.001$; Figure 5B). Moreover, the CAVBPH intervention recovered the collagen fibers in the diabetic wound tissues to the NC level, which was superior to

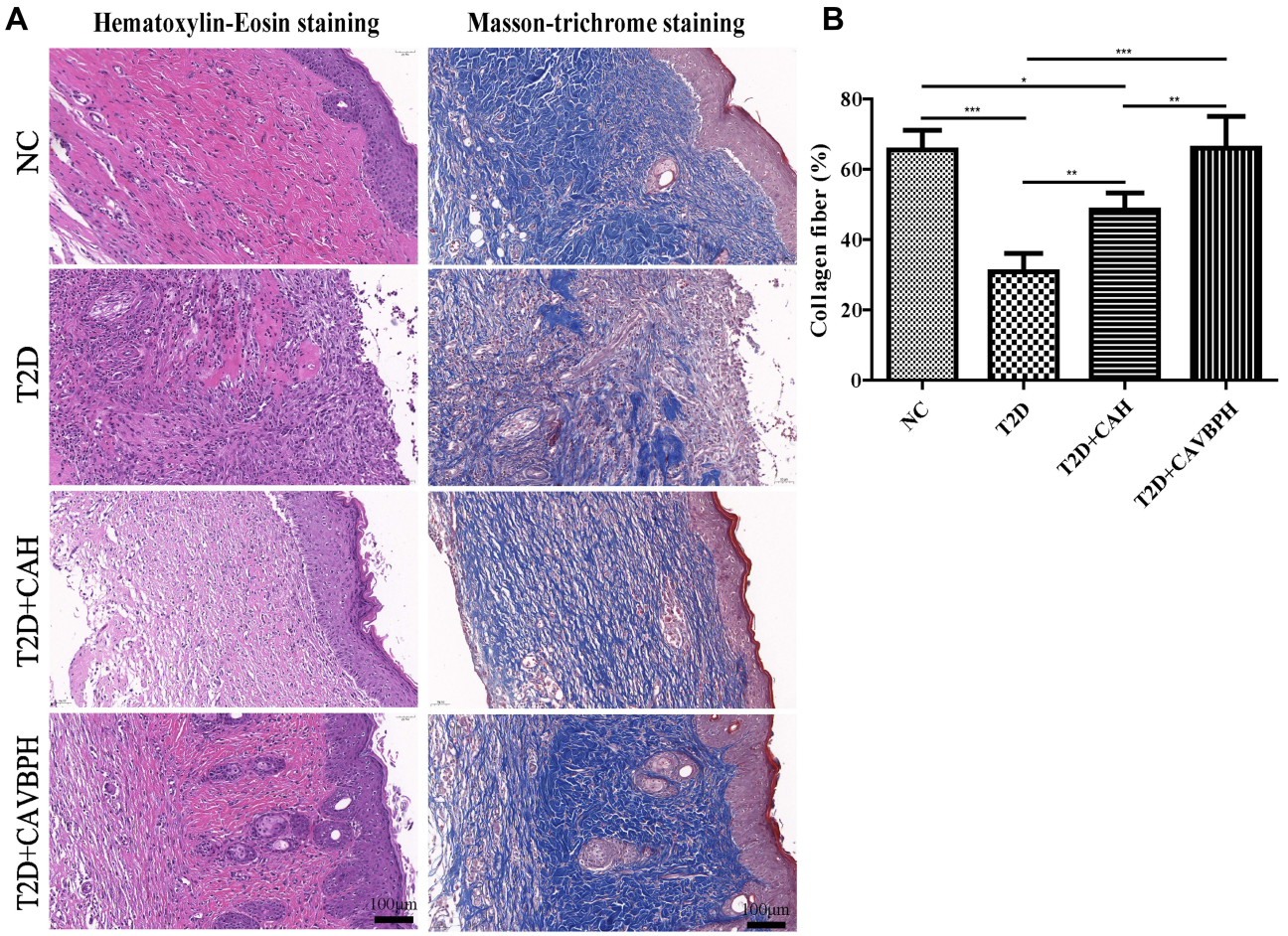

Figure 5 Histopathological staining of skin wounds in the normal control (NC) group, T2D group, CAH (T2D+CAH) group, and CAVBPH (T2D+CAVBPH) group on day 14. (**A**) Representative H&E and Masson staining images (scale bar = 100 μm). (**B**) Quantitative analysis of collagen fiber. *$p < 0.05$, **$p < 0.01$, and ***$p < 0.001$.

the CAH treatment ($p < 0.01$). These results provided evidence that CAVBPH treatment accelerates diabetic wound healing by regulating inflammation and promoting re-epithelialization, angiogenesis, and collagen deposition.

CAVBPH Up-Regulated CD31, PCNA, and α-SMA Proteins but Down-Regulated CD68 Expression in Wound

CD31, a marker of vascular endothelial cells, was used to assess new capillaries during wound healing. PCNA is one of the most prominent markers for cell proliferation,[37] while α-SMA is considered to be directly linked to the production of extracellular matrix (ECM) proteins.[38] In the current study, the expression of CD31, PCNA, and α-SMA in the T2D group was poorer than that in the NC group ($p < 0.001$; Figure 6). Conversely, these proteins were significantly up-regulated in the CAVBPH group compared with the T2D group ($p < 0.01$ or $p < 0.001$). CD68 is a glycoprotein highly expressed on monocytes and macrophages, especially during the inflammatory phase of skin wounds.[39] Treatment with CAH or CAVBPH dramatically suppressed the abnormal expression of CD68 protein in T2D wound tissue ($p < 0.001$). These results suggested that hydrogel treatment, especially CAVBPH, could up-regulate CD31, PCNA, and α-SMA proteins, while down-regulating CD68 expression, i.e., promote angiogenesis, cell proliferation, and ECM secretion as well as alleviate persistent inflammation during T2D wound healing.

CAVBPH Activated the PI3K/AKT/mTOR/HIF-1α/VEGFA Signaling Pathway

According to the results of bioinformatics analysis (Figure 3), we speculated that the PI3K/AKT and HIF-1 pathways might have a great potential effect on the healing of T2D wounds, thus the relative expression of active factors related to the PI3K/AKT/mTOR/HIF-1α/VEGFA pathway in wound tissue was further detected. As displayed in Figure 7A–D, the phosphorylation levels

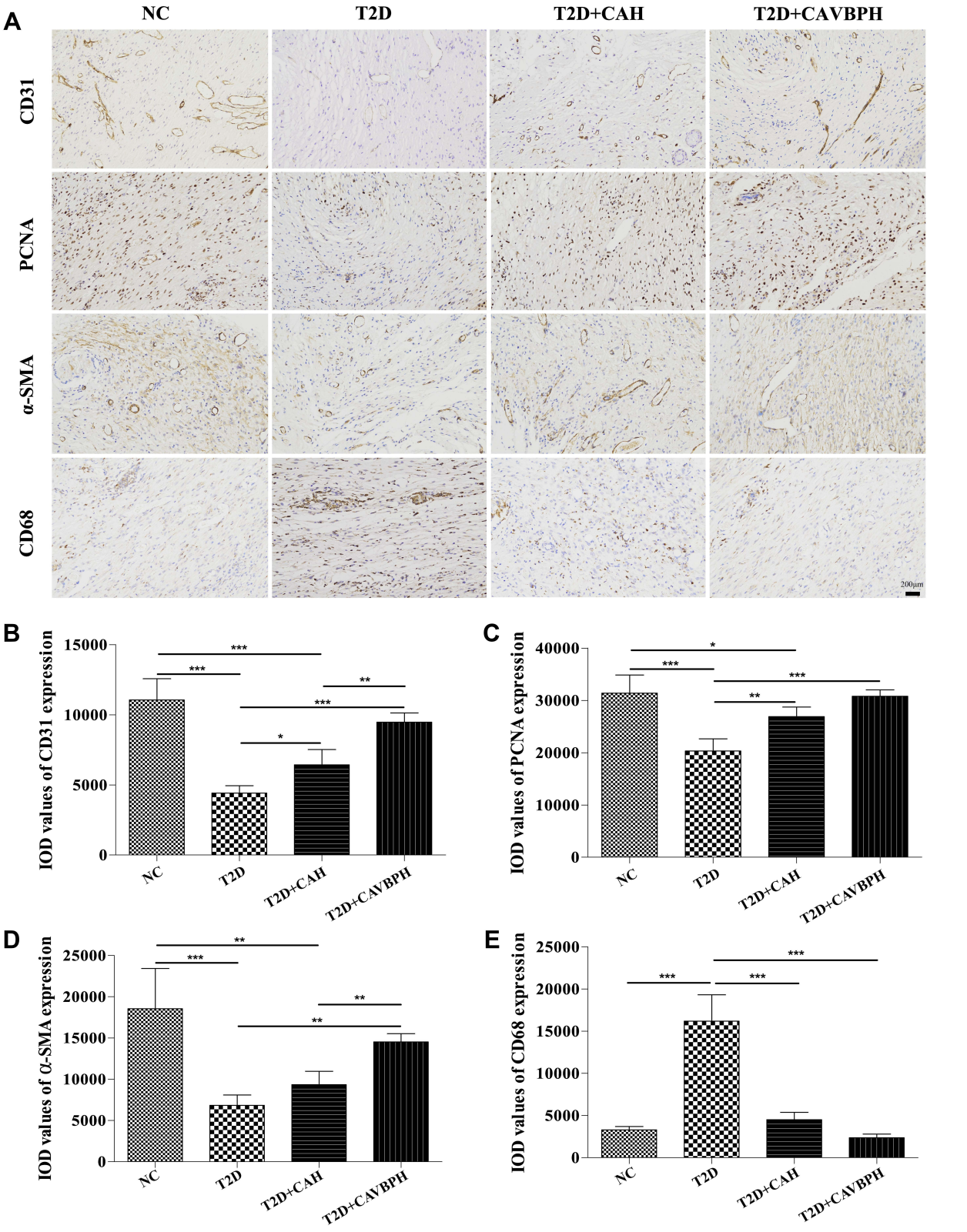

Figure 6 IHC staining of CD31, PCNA, α-SMA, and CD68 proteins. (**A**) Representative images for CD31, PCNA, α-SMA, and CD68 (scale bar = 200 μm). (**B**–**E**) Quantification analysis of CD31, PCNA, α-SMA, and CD68 proteins expression in wound tissues, respectively. *$p < 0.05$, **$p < 0.01$, and ***$p < 0.001$.

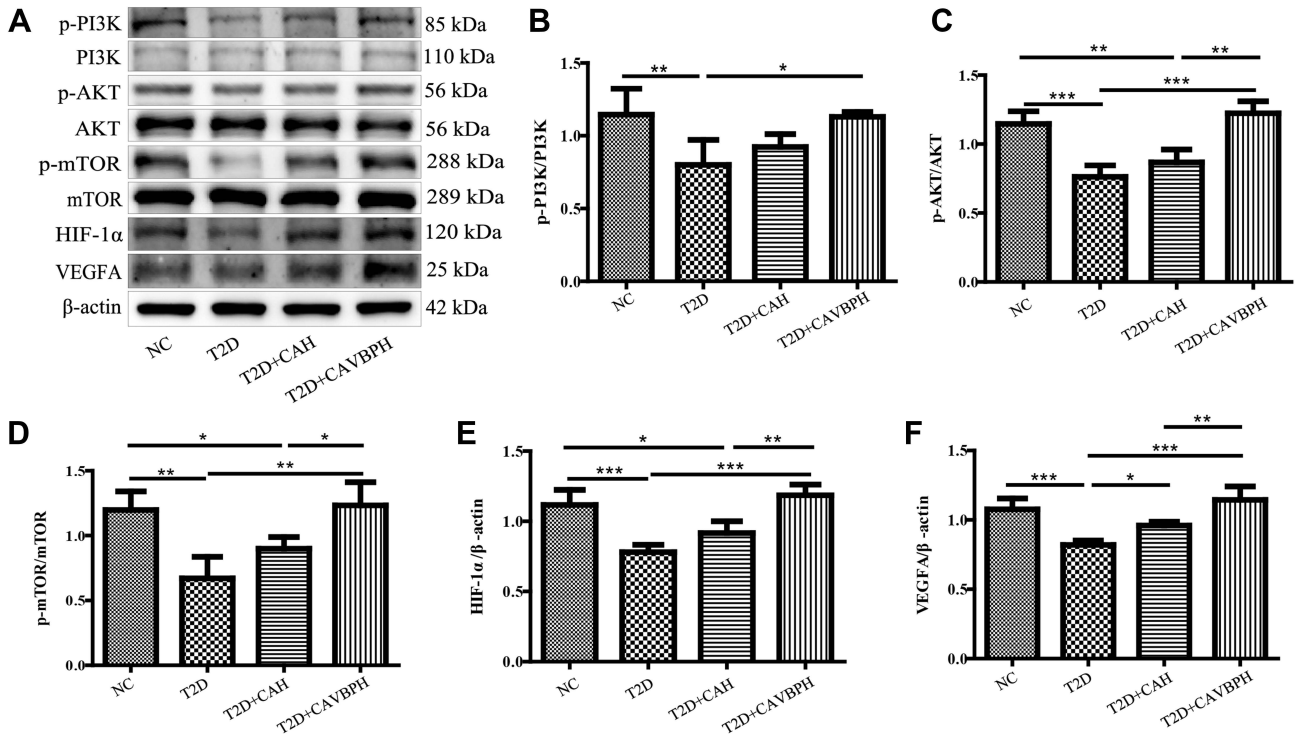

Figure 7 Western blot analysis of PI3K/AKT/mTOR/HIF-1α/VEGFA pathway. (**A**) Representative protein bands for p-PI3K, PI3K, p-AKT, AKT, p-mTOR, mTOR, HIF-1α, VEGFA, and β-actin. (**B**–**F**) Quantification analysis of p-PI3K/PI3K, p-AKT/AKT, p-mTOR/mTOR, HIF-1α/β-actin, and VEGFA/β-actin, respectively. *$p < 0.05$, **$p < 0.01$, and ***$p < 0.001$.

of PI3K, AKT, and mTOR proteins in the T2D group were noticeably lower than in the NC group ($p < 0.01$ or $p < 0.001$). Conversely, the CAVBPH treatment elevated the relative expression of p-PI3K/PI3K, p-AKT/AKT, and p-mTOR/mTOR in diabetic wounds ($p < 0.05$, $p < 0.01$, or $p < 0.001$), demonstrating that the CAVBPH activated the PI3K/AKT/mTOR pathway. We also found that T2D hindered the expression of downstream molecules HIF-1α and VEGFA in skin wound tissues ($p < 0.001$), whereas the CAVBPH intervention elevated the relative expression levels of these ($p < 0.001$; Figure 7A, E, and F). Unfortunately, we did not identify significant differences in the expression of the aforementioned proteins between the CAH group and the T2D group, except for VEGFA ($p < 0.05$). The above data proved that the CAVBPH activated the PI3K/AKT/mTOR/HIF-1α/VEGFA pathway in vivo, which contributed to the rapid healing of diabetic wounds.

CAVBPH Inhibited the Overexpression of Inflammatory Factors

To investigate the inflammatory response of T2D wounds, we detected the protein expression of inflammatory cytokines IL-1β and TNF-α by Western blot based on the results of bioinformatics analysis. As presented in Figure 8, the relative expression of TNF-α and IL-1β in the T2D group was dramatically risen as compared to the NC group ($p < 0.001$). However, CAH and CAVBPH treatments significantly reduced the expression levels of IL-1β and TNF-α in T2D wound tissues ($p < 0.05$, $p < 0.01$, or $p < 0.001$). In addition, the CAVBPH intervention remarkably down-regulated the expression of IL-1β and TNF-α when compared with the CAH group ($p < 0.01$). This was consistent with the CD68 staining results, that is, CS/SA hydrogel loaded with VBPs was beneficial for reducing the inflammation level at T2D wound sites.

CAVBPH Restored the Diversity and Structure of Skin Microbiota at T2D Wounds

The rarefaction curve and species accumulation curve showed that the increase of species numbers tended to flatten with the increase of sequencing depth and samples, respectively, indicating that the data quality and sample number were sufficient (Figure S2). The number of OTUs is regarded as an index reflecting the abundance of microbial species in the samples. As presented in Figure 9A, 3989, 3627, 3110, and 3879 OTUs were in the NC, T2D, CAH, and CAVBPH groups, respectively. 350 OTUs were co-overlapping in the above four groups. α-diversity, which reflects the richness

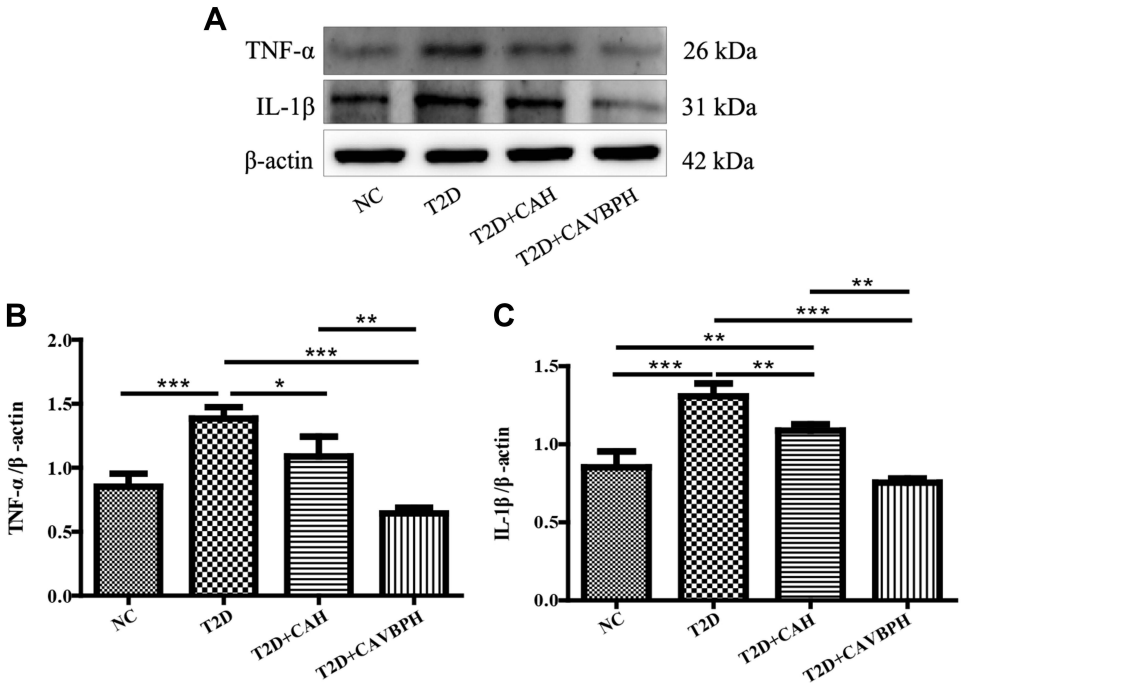

Figure 8 Western blot analysis of inflammatory factors TNF-α and IL-1β proteins. (**A**) Representative protein bands for TNF-α, IL-1β, and β-actin. (**B** and **C**) Quantification analysis of TNF-α/β-actin and IL-1β/β-actin. *p < 0.05, **p < 0.01, and ***p < 0.001.

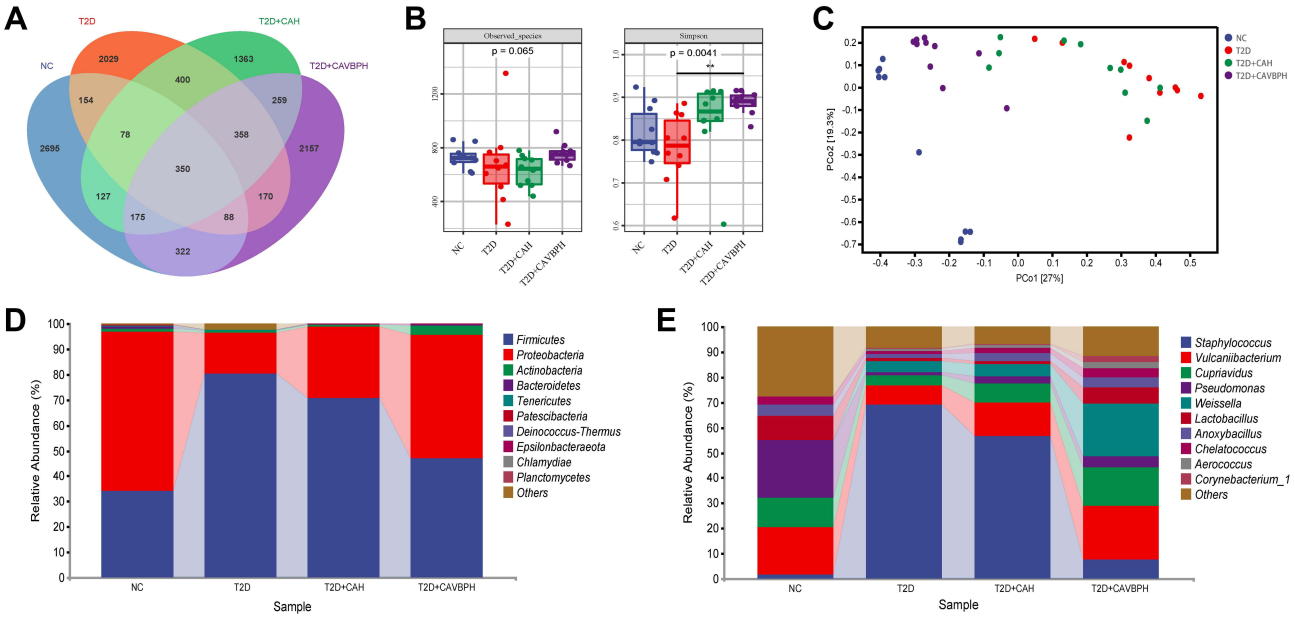

Figure 9 16S rRNA sequencing of skin flora in mice. (**A**) Venn diagrams of operational taxonomic units (OTUs) in the NC, T2D, CAH (T2D+CAH), and CAVBPH (T2D +CAVBPH) groups. (**B**) α-diversity analysis. (**C**) β-diversity analysis. (**D**) Relative abundance of community at the phylum level. (**E**) Percent of community abundance at the genus level. **p < 0.01.

and diversity of each sample species, was assessed by the Observed species index and the Simpson index (Figure 9B). The results showed that T2D caused a decrease in the α-diversity of skin microbiota, whereas the CAVBPH intervention increased the Observed species (p = 0.065) and Simpson (p = 0.0041) indices when compared with the T2D group. Principal coordinate analysis represents the community differences between groups and reflects the β-diversity of

microflora. As shown in Figure 9C, the sample clustering of the T2D group was significantly far away from the NC group. Community differences began to appear between the CAH group and the T2D group, and the CAVBPH group was clearly separated from the T2D group and had the smallest differences with NC mice.

The dominant bacteria among the four groups, at the phylum level, were *Firmicutes, Proteobacteria, Actinobacteria*, and *Bacteroidetes*. The relative abundance of *Firmicutes, Proteobacteria, Actinobacteria*, and *Bacteroidetes* in the NC group was 34.05%, 62.63%, 1.46%, and 0.85%, respectively. Compared to the NC group, the relative abundance of *Firmicutes* (80.22%) was increased, while the relative levels of *Proteobacteria* (16.13%), *Actinobacteria* (0.90%), and *Bacteroidetes* (0.09%) were down-regulated in the T2D group. The relative abundance of *Proteobacteria* (28.21%) and *Bacteroidetes* (0.11%) was increased, but *Firmicutes* (70.52%) was decreased in the CAH group when compared with the T2D group. In the CAVBPH group, the relative abundance of *Firmicutes* (46.96%) was lower while the relative contents of *Proteobacteria* (48.79%), *Actinobacteria* (3.47%), and *Bacteroidetes* (0.30%) were higher than the T2D group. *Firmicutes* are normally seen as harmful microorganisms that disrupt lipid and glucose metabolism, and a high ratio of *Firmicutes* to *Bacteroidetes* (F: B ratio) is thought to be linked to an increased risk of T2D.[40] Meanwhile, CAVBPH treatment significantly reduced the F: B ratio of T2D mice from 891.3 to 156.5. At the genus level, the relative abundance of *Staphylococcus* (69.08%) and *Weissella* (4.33%) in the T2D group displayed a significant elevation (1.72% and 0.27% in the NC group, respectively), but the relative abundance of *Vulcaniibacterium* (7.59%), *Cupriavidus* (4.19%), *Pseudomonas* (1.01%), *Lactobacillus* (1.48%), *Anoxybacillus* (1.53%), *Chelatococcus* (1.03%), *Aerococcus* (0.73%), and *Corynebacterium_1* (0.68%) was decreased (18.78%, 11.61%, 22.74%, 9.58%, 4.53%, 2.92%, 0.12%, and 0.22% in the NC group, respectively). CAVBPH treatment remarkably reversed T2D-induced skin flora dysregulation at the genus level, except for the up-regulation of *Weissella* in relative abundance. These changes in skin flora may be important pathways by which diabetic wounds maintain long-time ulcers and CAVBPH promotes skin tissue repair.

Spearman Correlation Between Skin Microbiota and Active Proteins in Diabetic Wounds

Spearman heatmap showed significant correlations between the dominant skin microbes around diabetic wounds and factors related to angiogenesis and inflammation in the tissue during topical application of CAVBPH (Figure 10). At the phylum level, *Firmicutes* were negatively correlated with p-PI3K/PI3K, p-AKT/AKT, p-mTOR/mTOR, HIF-1α, and

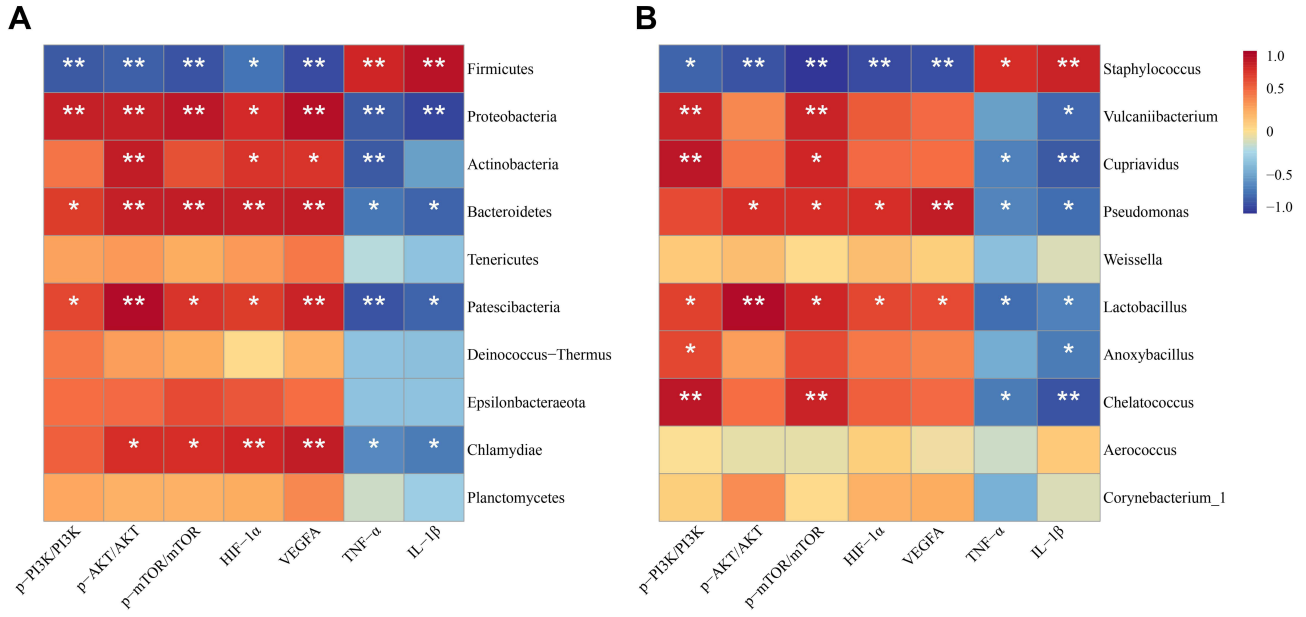

Figure 10 Spearman correlation analysis between skin microbiota and active proteins related to angiogenesis and inflammation in diabetic wounds. (**A**) Correlation heatmap of skin microbes and active proteins at the phylum level. (**B**) Correlation heatmap of skin microbes and active proteins at the genus level. *$p < 0.05$ and **$p < 0.01$.

VEGFA, but positively related to IL-1β and TNF-α ($p < 0.05$ or $p < 0.01$); conversely, *Proteobacteria, Bacteroidetes*, and *Patescibacteria* were positively associated with the PI3K/AKT/mTOR/HIF-1α/VEGFA pathway-related factors, but negatively correlated with inflammatory cytokines IL-1β and TNF-α ($p < 0.05$ or $p < 0.01$; Figure 10A). To obtain more information, we further calculated the spearman coefficient at the genus level (Figure 10B). Specifically, *Staphylococcus* was negatively correlated with the expression of related proteins of the PI3K/AKT/mTOR/HIF-1α/VEGFA pathway, while positively related to IL-1β and TNF-α ($p < 0.05$ or $p < 0.01$). *Lactobacillus* was observed to have an opposite correlation trend to *Staphylococcus*. In addition, *Vulcaniibacterium, Cupriavidus, Pseudomonas, Anoxybacillus*, and *Chelatococcus* were also strongly associated with the expression of angiogenesis and inflammation-related factors. Thus, these skin microbes were indirectly or directly linked to the therapeutic ability of CAVBPH on T2D wounds by the skin flora-active proteins axis.

Discussion

Skin wound is a common chronic complication of diabetes and one of the leading factors that threaten the physical and mental health of diabetic patients and cause serious economic and social burdens.[1–3] Therefore, it is a pressing need to investigate the pathogenesis and effective strategies for delayed wound healing. Studies have reported that bioactive peptides-loaded hydrogels are a promising option for repairing tissue damage.[16,20,21,26] Velvet antler has regenerative property, and both velvet antler and velvet antler peptides have been proved to have wound repair activity.[19,41] VB derived from velvet antler is rich in proteins and peptides, and TCM believes that its activity is similar to that of velvet antler. In this study, we encapsulated short-chain VBPs with antioxidant activity in a CS/SA hydrogel scaffold and explored its efficacy on T2D skin wound repair for the first time.

Previously, CS/SA polymer was shown to be more efficient in promoting wound repair than either CS or SA alone, and CS/SA composite hydrogel possessed excellent physicochemical properties to support it as a promising wound dressing scaffold.[25,42] The results of in vitro evaluation showed that CAVBPH possessed good porous breathability, swelling, biodegradability, antioxidant property, biocompatibility, biosafety, and release behavior of VBPs (Figures 1 and 2). Subsequently, we topically applied CAVBPH to the wound surface, on the one hand, to avoid direct contact of the wound with the outside, and on the other hand to continuously provide VBPs for wound healing. Compared to the T2D and CAH groups, the CAVBPH group had the best curative effect, with a 96.55% wound healing rate on day 15 (Figure 4). Pathological staining revealed the positive influence of CAVBPH on angiogenesis, re-epithelialization, fibroblast proliferation, collagen deposition, and inflammation regulation (Figures 5 and 6). We also found that the therapeutic effect of CAVBPH on T2D skin wounds was better than recently reported CS-based hydrogels, decellularized skin scaffolds, and herbal ointments based on a literature review.[16,17,31,43] However, the specific mechanism by which CAVBPH exerts its efficacy remains unknown.

Bioinformatics studies can comprehensively analyze genome-wide profiles of clinical samples and have been extensively applied to explore the pathogenesis and promising therapeutic targets in various diseases.[44,45] In this study, bioinformatics analysis found that diabetic wound-specific DEGs were significantly correlated with the PI3K/AKT and HIF-1 signaling pathways (Figure 3). HIF-1α is a vital molecule regulating angiogenesis and is a downstream node of the PI3K/AKT/mTOR pathway. Excessive glucose levels interfere with the activity and stability of HIF-1α, resulting in the failure of VEGFA up-regulation in diabetic wounds, which in turn causes impaired angiogenesis and wound healing.[46] CS-based wound dressings have been shown to exert therapeutic effects by activating the PI3K/AKT pathway.[25,47] Interestingly, this work confirmed that CAVBPH more prominently exerted a pro-angiogenic effect than CAH via activating the PI3K/AKT/mTOR/HIF-1α/VEGFA pathway (Figure 7).

The development of DFU is accompanied by persistent chronic inflammation. Accumulating evidence suggests that inflammatory responses mediated by IL-1β and TNF-α damage vascular endothelial cells and weaken insulin sensitivity, causing defects in wound healing. On the contrary, silencing TNF-α or blocking IL-1β can effectively improve the healing of DFU by inducing macrophages to polarize into healing-related phenotypes and inhibiting macrophage infiltration.[48,49] In this study, CAVBPH intervention significantly down-regulated the levels of IL-1β, TNF-α, and CD68, indicating that CAVBPH had a good therapeutic effect on chronic inflammation of T2D wounds (Figures 6 and 8).

Skin flora is considered critical for protecting humans from pathogens and maintaining the balance of the immune system. Currently, whether topical application of skin dressings can improve skin ulcers by affecting the microflora around diabetic wounds requires further investigation. It is reported that low microflora diversity was associated with some metabolic disorders, while higher overall diversity meant better health.[50,51] Our results showed that CAVBPH therapy reversed the poor diversity and structure of skin flora induced by T2D and made them tend to a healthy level (Figure 9). Skin symbiotic bacteria *Cutibacterium* and *Corynebacterium* contained genes related to porphyrin metabolism, which could theoretically reduce infections caused by *Staphylococcus aureus*.[52] In addition, a variety of *Lactobacillus* species have been reported as beneficial bacteria for the prevention and treatment of gastrointestinal and genitourinary system infections. Live *Lactobacillus reuteri* DSM 17938 was found to have an inhibitory effect on skin pathogenic bacteria (*Pseudomonas aeruginosa, Cutibacterium acnes AS12, Streptococcus pyogenes M1*, and *Staphylococcus aureus*).[53] CAVBPH dramatically increased the relative abundance of *Corynebacterium_1* and *Lactobacillus* at the genus level, suggesting the effectiveness of CAVBPH in chronic wounds and the correlation between the regulation of skin microbiota and the improvement of skin ulcers. Moreover, we believe that the purposeful regulation and improvement of skin microbiota will facilitate the clinical treatment of diabetic wounds. Interestingly, we also noticed that changes in the relative abundance of some dominant microorganisms were significantly associated with the efficacy of CAVBPH in enhancing angiogenesis and alleviating persistent inflammation. However, further studies must be performed to analyze the exact biological mechanism by which CAVBPH improves diabetic wound healing through the skin flora-active protein axis.

Conclusion

This is the first study to widely analyze the therapeutic effect of VBPs delivered to T2D skin wounds using a CS/SA hydrogel scaffold, which provides novel insights into the modern application of VBPs and the treatment of diabetic ulcer. The results suggest that CAVBPH, as a promising alternative therapy for diabetic wounds, could promote angiogenesis and cell proliferation and alleviate inflammation via activating the PI3K/AKT/mTOR/HIF-1α/VEGFA pathway and reversing the expression of TNF-α and IL-1β. Also, CAVBPH restored the diversity and structure of T2D skin flora. The excellent therapeutic efficacy of CAVBPH on chronic cutaneous trauma may be related to numerous short-chain VBPs, which needs further study.

Acknowledgments

We sincerely acknowledge Yiwen Zhang, Shuang Ma, Qiteng Ding, Jinping Zhang, and Huiying Chen from Jilin Agricultural University for their help under our guidance.

Funding

This research was supported by the Jilin Province Science and Technology Development Plan Project (20220401071YY).

Disclosure

The authors report no conflicts of interest in this work.

References

1. Krug EG. Trends in diabetes: sounding the alarm. *Lancet*. 2016;387(10027):1485–1486. doi:10.1016/S0140-6736(16)30163-5
2. Basu S, Yudkin JS, Kehlenbrink S, et al. Estimation of global insulin use for type 2 diabetes, 2018–30: a microsimulation analysis. *Lancet Diabetes Endocrinol*. 2019;7(1):25–33. doi:10.1016/S2213-8587(18)30303-6
3. Brem H, Tomic-Canic M. Cellular and molecular basis of wound healing in diabetes. *J Clin Investig*. 2007;117(5):1219–1222. doi:10.1172/JCI32169
4. Holl J, Kowalewski C, Zimek Z, et al. Chronic diabetic wounds and their treatment with skin substitutes. *Cells*. 2021;10(3):655. doi:10.3390/cells10030655
5. Sun BK, Siprashvili Z, Khavari PA. Advances in skin grafting and treatment of cutaneous wounds. *Science*. 2014;346(6212):941–945. doi:10.1126/science.1253836
6. Lou P, Liu S, Xu X, Pan C, Lu Y, Liu J. Extracellular vesicle-based therapeutics for the regeneration of chronic wounds: current knowledge and future perspectives. *Acta Biomaterialia*. 2021;119:42–56. doi:10.1016/j.actbio.2020.11.001

7. Hyldig K, Riis S, Pennisi CP, Zachar V, Fink T. Implications of extracellular matrix production by adipose tissue-derived stem cells for development of wound healing therapies. *Int J Molecul Sci*. 2017;18(6):1167. doi:10.3390/ijms18061167
8. Yang Y, Zhao X, Yu J, et al. Bioactive skin-mimicking hydrogel band-aids for diabetic wound healing and infectious skin incision treatment. *Bioactive Material*. 2021;6(11):3962–3975. doi:10.1016/j.bioactmat.2021.04.007
9. Xu Z, Han S, Gu Z, Wu J. Advances and impact of antioxidant hydrogel in chronic wound healing. *Adv Healthcare Material*. 2020;9(5):1901502. doi:10.1002/adhm.201901502
10. Shariatinia Z. Pharmaceutical applications of chitosan. *Adv Colloid Interface Sci*. 2019;263:131–194. doi:10.1016/j.cis.2018.11.008
11. Rao SB, Sharma CP. Use of chitosan as a biomaterial: studies on its safety and hemostatic potential. *J Biomed Material Res*. 1997;34(1):21–28. doi:10.1002/(SICI)1097-4636(199701)34:1<21::AID-JBM4>3.0.CO;2-P
12. Zhang M, Zhao X. Alginate hydrogel dressings for advanced wound management. *Int J Biological Macromol*. 2020;162:1414–1428. doi:10.1016/j.ijbiomac.2020.07.311
13. Zang S, Mu R, Chen F, et al. Injectable chitosan/β-glycerophosphate hydrogels with sustained release of BMP-7 and ornidazole in periodontal wound healing of class III furcation defects. *Materials Sci Eng*. 2019;99:919–928. doi:10.1016/j.msec.2019.02.024
14. Asfour MH, Abd El-Alim SH, Awad GEA, Kassem AA. Chitosan/β-glycerophosphate in situ forming thermo-sensitive hydrogel for improved ocular delivery of moxifloxacin hydrochloride. *Euro J Pharmaceuti Sci*. 2021;167:106041. doi:10.1016/j.ejps.2021.106041
15. Zhou P, Li X, Zhang B, Shi Q, Li D, Ju X. A human umbilical cord mesenchymal stem cell-conditioned medium/chitosan/collagen/β-glycerophosphate thermosensitive hydrogel promotes burn injury healing in mice. *BioMed Res Int*. 2019;2019:5768285. doi:10.1155/2019/5768285
16. Zhang D, Ouyang Q, Hu Z, et al. Catechol functionalized chitosan/active peptide microsphere hydrogel for skin wound healing. *Int J Biol Macromol*. 2021;173:591–606. doi:10.1016/j.ijbiomac.2021.01.157
17. Wei L, Tan J, Li L, et al. Chitosan/alginate hydrogel dressing loaded FGF/VE-cadherin to accelerate full-thickness skin regeneration and more normal skin repairs. *Int J Mol Sci*. 2022;23(3):1249. doi:10.3390/ijms23031249
18. Huang Y, Yang N, Teng D, et al. Antibacterial peptide NZ2114-loaded hydrogel accelerates Staphylococcus aureus-infected wound healing. *Appl Microbiol Biotechnol*. 2022;106(9–10):3639–3656. doi:10.1007/s00253-022-11943-w
19. Gu L, Mo E, Yang Z, et al. Effects of red deer antlers on cutaneous wound healing in full-thickness rat models. *Asian-Australas J Anim Sci*. 2008;21(2):277–290. doi:10.5713/ajas.2008.70348
20. Zhang Z, Zhao M, Wang J, Ding Y, Dai X, Li Y. Oral administration of skin gelatin isolated from chum salmon (oncorhynchus keta) enhances wound healing in diabetic rats. *Mar Drugs*. 2011;9(5):696–711. doi:10.3390/md9050696
21. Ouyang -Q-Q, Hu Z, Lin Z-P, et al. Chitosan hydrogel in combination with marine peptides from tilapia for burns healing. *Int J Biol Macromol*. 2018;112:1191–1198. doi:10.1016/j.ijbiomac.2018.01.217
22. Tseng S-H, Sung H-C, Chen L-G, et al. Effects of velvet antler with blood on bone in ovariectomized rats. *Molecules*. 2012;17(9):10574–10585. doi:10.3390/molecules170910574
23. Lv -J-J, Liu Y, Zeng X-Y, et al. Anti-fatigue peptides from the enzymatic hydrolysates of cervus elaphus blood. *Molecules*. 2021;26(24):7614. doi:10.3390/molecules26247614
24. Ma L, Le G, Qian J, Jiang H, Shi Y. Preparation and bioactivity of immunopeptide from cervus-elaphus linnaeas antler blood. *Nat Prod Res Develop*. 2009;21(1):125–182.
25. Hao M, Peng X, Sun S, Ding C, Liu W. Chitosan/sodium alginate/velvet antler blood peptides hydrogel promoted wound healing by regulating PI3K/AKT/mTOR and SIRT1/NF-κB pathways. *Front Pharmacol*. 2022;13:913408.
26. Zhang D, Hu Z, Zhang L, Lu S, Liang F, Chitosan-Based Thermo-Sensitive LS. Hydrogel loading oyster peptides for hemostasis application. *Materials*. 2020;13(21):5038. doi:10.3390/ma13215038
27. Abueva CDG, Lee B-T. Poly(vinylphosphonic acid) immobilized on chitosan: a glycosaminoglycan-inspired matrix for bone regeneration. *Int J Biol Macromol*. 2014;64:294–301. doi:10.1016/j.ijbiomac.2013.12.018
28. Xu C, Guan S, Xu J, et al. Preparation, characterization and antioxidant activity of protocatechuic acid grafted carboxymethyl chitosan and its hydrogel. *Carbohydr Polym*. 2021;252:117210. doi:10.1016/j.carbpol.2020.117210
29. Sun S, Hao M, Ding C, et al. SF/PVP nanofiber wound dressings loaded with phlorizin: preparation, characterization, in vivo and in vitro evaluation. *Biointerfaces*. 2022;217:112692. doi:10.1016/j.colsurfb.2022.112692
30. Ritchie ME, Phipson B, Wu D, et al. limma powers differential expression analyses for RNA-sequencing and microarray studies. *Nucleic Acids Res*. 2015;43(7):e47–e47. doi:10.1093/nar/gkv007
31. Liu H, Liu H, Deng X, et al. CXCR4 antagonist delivery on decellularized skin scaffold facilitates impaired wound healing in diabetic mice by increasing expression of SDF-1 and enhancing migration of CXCR4-positive cells. *Wound Repair Regen*. 2017;25(4):652–664. doi:10.1111/wrr.12552
32. Wang G, Wang X, Huang L. Feasibility of chitosan-alginate (Chi-Alg) hydrogel used as scaffold for neural tissue engineering: a pilot study in vitro. *Biotechnol Biotechnol Equip*. 2017;31(4):766–773. doi:10.1080/13102818.2017.1332493
33. Cui H, Cui L, Zhang P, Huang Y, Wei Y, Chen X. In situ electroactive and antioxidant supramolecular hydrogel based on cyclodextrin/copolymer inclusion for tissue engineering repair. *Macromol Biosci*. 2014;14(3):440–450. doi:10.1002/mabi.201300366
34. Bölgen N, Demir D, Yalçın MS, Özdemir S. Development of Hypericum perforatum oil incorporated antimicrobial and antioxidant chitosan cryogel as a wound dressing material. *Int J Biol Macromol*. 2020;161:1581–1590. doi:10.1016/j.ijbiomac.2020.08.056
35. Hu S, Bi S, Yan D, et al. Preparation of composite hydroxybutyl chitosan sponge and its role in promoting wound healing. *Carbohydr Polym*. 2018;184:154–163. doi:10.1016/j.carbpol.2017.12.033
36. Yang X, Yang K, Wu S, et al. Cytotoxicity and wound healing properties of PVA/ws-chitosan/glycerol hydrogels made by irradiation followed by freeze–thawing. *Radiat Phys Chem*. 2010;79(5):606–611. doi:10.1016/j.radphyschem.2009.12.017
37. Elmowafy M, Shalaby K, Salama A, et al. Soy isoflavone-loaded alginate microspheres in thermosensitive gel base: attempts to improve wound-healing efficacy. *J Pharm Pharmacol*. 2019;71(5):774–787. doi:10.1111/jphp.13066
38. Elbialy ZI, Assar DH, Abdelnaby A, et al. Healing potential of Spirulina platensis for skin wounds by modulating bFGF, VEGF, TGF-ß1 and α-SMA genes expression targeting angiogenesis and scar tissue formation in the rat model. *Biomed Pharmacother*. 2021;137:111349. doi:10.1016/j.biopha.2021.111349
39. Yang Y, Liang Y, Chen J, Duan X, Guo B. Mussel-inspired adhesive antioxidant antibacterial hemostatic composite hydrogel wound dressing via photo-polymerization for infected skin wound healing. *Bioactive Material*. 2022;8:341–354. doi:10.1016/j.bioactmat.2021.06.014

40. Song Y, Wu M-S, Tao G, Lu M-W, Lin J, Huang J-Q. Feruloylated oligosaccharides and ferulic acid alter gut microbiome to alleviate diabetic syndrome. *Food Res Int*. 2020;137:109410. doi:10.1016/j.foodres.2020.109410
41. Zha E, Gao S, Pi Y, Li X, Wang Y, Yue X. Wound healing by a 3.2 kDa recombinant polypeptide from velvet antler of Cervusnippon Temminck. *Biotechnol Lett*. 2012;34(4):789–793. doi:10.1007/s10529-011-0829-8
42. Zhao W-Y, Fang -Q-Q, Wang X-F, et al. Chitosan-calcium alginate dressing promotes wound healing: a preliminary study. *Wound Repair Regen*. 2020;28(3):326–337. doi:10.1111/wrr.12789
43. Gharaboghaz M, Farahpour MR, Saghaie S. Topical co-administration of Teucrium polium hydroethanolic extract and Aloe vera gel triggered wound healing by accelerating cell proliferation in diabetic mouse model. *Biomed Pharmacother*. 2020;127:110189. doi:10.1016/j.biopha.2020.110189
44. Hao M, Liu W, Ding C, et al. Identification of hub genes and small molecule therapeutic drugs related to breast cancer with comprehensive bioinformatics analysis. *PeerJ*. 2020;8:e9946. doi:10.7717/peerj.9946
45. Allison DB, Cui X, Page GP, Sabripour M. Microarray data analysis: from disarray to consolidation and consensus. *Nat Rev Genet*. 2006;7(1):55–65. doi:10.1038/nrg1749
46. Thangarajah H, Vial IN, Grogan RH, et al. HIF-1α dysfunction in diabetes. *Cell Cycle*. 2010;9(1):75–79. doi:10.4161/cc.9.1.10371
47. Wang X-F, Li M-L, Fang -Q-Q, et al. Flexible electrical stimulation device with Chitosan-Vaseline® dressing accelerates wound healing in diabetes. *Bioactive Material*. 2021;6(1):230–243. doi:10.1016/j.bioactmat.2020.08.003
48. Kasiewicz LN, Whitehead KA. Silencing TNFα with lipidoid nanoparticles downregulates both TNFα and MCP-1 in an in vitro co-culture model of diabetic foot ulcers. *Acta Biomaterialia*. 2016;32:120–128. doi:10.1016/j.actbio.2015.12.023
49. Mirza RE, Fang MM, Ennis WJ, Koh TJ. Blocking interleukin-1β induces a healing-associated wound macrophage phenotype and improves healing in type 2 diabetes. *Diabetes*. 2013;62(7):2579–2587. doi:10.2337/db12-1450
50. Doré J, Blottière H. The influence of diet on the gut microbiota and its consequences for health. *Curr Opin Biotechnol*. 2015;32:195–199. doi:10.1016/j.copbio.2015.01.002
51. Zhu J, Wu M, Zhou H, Cheng L, Wei X, Wang Y. Liubao brick tea activates the PI3K-Akt signaling pathway to lower blood glucose, metabolic disorders and insulin resistance via altering the intestinal flora. *Food Res Int*. 2021;148:110594. doi:10.1016/j.foodres.2021.110594
52. Orenstein A, Klein D, Kopolovic J, et al. The use of porphyrins for eradication of Staphylococcus aureus in burn wound infections. *FEMS Immunol Med Microbiol*. 1997;19(4):307–314. doi:10.1111/j.1574-695X.1997.tb01101.x
53. Khmaladze I, Butler É, Fabre S, Gillbro JM. Lactobacillus reuteri DSM 17938—A comparative study on the effect of probiotics and lysates on human skin. *Exp Dermatol*. 2019;28(7):822–828. doi:10.1111/exd.13950